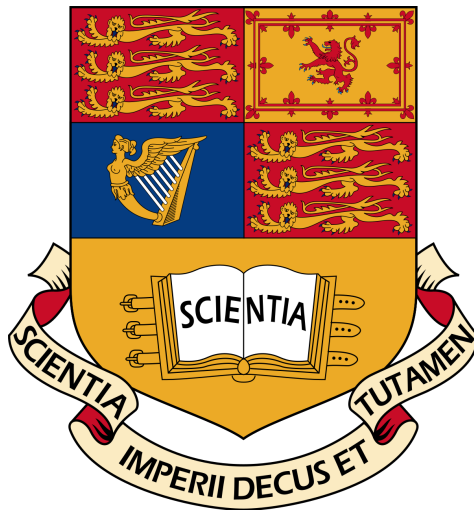


# INVESTIGATING THE USE OF PHENOMENOLOGICAL AND MECHANISTIC MODELS TO FIT THE THERMAL RESPONSES OF METABOLIC TRAITS

Eva Linehan



Computational Methods in Ecology and Evolution

Miniproject

Imperial College London

March 2019

WC 1924

# Contents

<b>1</b>	<b>Abstract</b>	<b>2</b>
<b>2</b>	<b>Introduction</b>	<b>2</b>
<b>3</b>	<b>Methods</b>	<b>4</b>
3.1	Data . . . . .	4
3.2	Model fitting . . . . .	4
3.2.1	Phenomenological Models . . . . .	4
3.2.2	Mechanistic Models . . . . .	5
3.3	Model Selection . . . . .	7
<b>4</b>	<b>Results</b>	<b>8</b>
<b>5</b>	<b>Discussion</b>	<b>15</b>
	<b>References</b>	<b>16</b>
<b>6</b>	<b>Appendices</b>	<b>20</b>
6.0.1	Appendix 1 . . . . .	20

# 1 Abstract

## 2 Introduction

3 It has been argued that life is a response to the thermodynamic requirements of dissi-  
4 pating systems, providing criteria for evaluating growth and development across a range  
5 of biological systems (Schneider & Kay, 2007). The importance of thermodynamic im-  
6 peratives in fluctuating environments and in ecosystem maintenance cannot be under-  
7 stated in this present climate. The most recent IPCC 2018 report (O.Hoegh-Guldberg  
8 et al., 2018) identified the investigation of thermal responses across terrestrial, coastal  
9 and oceanic ecosystems as crucial gap in our knowledge and in the understanding of  
10 mechanistic processes by which organisms react to Earth’s rapidly changing thermal  
11 landscape. To observe the profound effects of temperature on biological functions at  
12 all levels of organization, temperature performance curves are commonly used.

13 Temperature performance curves (TPCs) incorporate temperature tolerance and  
14 temperature-dependent effects on performance from the whole-organism level, includ-  
15 ing growth and metabolic rate, to the underlying physiological level which include  
16 functions such as enzyme activity (Fangue, Healy, & Schulte, 2011)(Dell, Pawar, &  
17 Savage, n.d.). The effects of temperature on performance traits, illustrated by TPCs,  
18 follow a general trend with three distinct phases: (1) a growth phase with trait per-  
19 formance increasing with temperature; (2) a peak or thermal optimum at the highest  
20 trait value; followed by (3) a sharp decline at higher temperatures (Schulte, 2015). This  
21 unimodal, left skewed distribution has been described by both phenomenological and  
22 mechanistic models in order to capture the general features observed for trait values  
23 across a range of temperatures. There is currently no one general model favoured over  
24 another which may be explained by the fundamental differences between biological re-  
25 sponses among taxa (Dell, Pawar, & Savage, 2011)(Low-Dălcărie et al., n.d.). An ideal

26 generalized model may be hard to derive as although complex models often perform  
27 poorly in relation to a more simple counterpart, they can be improved when wider  
28 temperature ranges are applied (Quinn, 2017). Phenomenological models, often used  
29 to predict thermal responses, lack any meaningful parameter interpretation and as a  
30 result are flexible tools that can be used to model any species or fitness component  
31 (Martin et al., 2017). The unknown suitability for such models in different conditions  
32 may lead to underestimation. In contrast, mechanistic models are used to explain the  
33 processes underlying phenomena in empirical data and are established on a theoretical  
34 basis. The mechanistic basis for model predictions provides a useful criterion in a range  
35 of applications, such as conservation assessments (Bernardo & Spotila, 2006).

36 Both phenomenological and mechanistic models were compared in this study to ana-  
37 lyze the effect of temperature on trait performance. Phenomenological models include; a  
38 cubic polynomial which is unimodal and asymmetrical in shape as well as Briere’s model  
39 that accounts for upper and lower temperature thresholds (Pracros, Briere, Le Roux, &  
40 Pierre, 1999). The mechanistic models chosen were variations of the Schoolfield-Sharpe  
41 model that consider reversible enzyme denaturation at high (S1), low temperatures (S2)  
42 or both (S3). Formulated from the Sharpe and DeMichele model which was unsuitable  
43 for non-linear regression, three new thermodynamic parameters were introduced which  
44 have a more intuitive biological interpretation: (1) a development rate at a reference  
45 temperature that assumes no enzyme activity; (2) a temperature at which enzyme ac-  
46 tivity is half low temperature inactive; and (3) a temperature at which enzyme activity  
47 is half high temperature inactive. (“Non-linear regression of biological temperature-  
48 dependent rate models based on absolute reaction-rate theory”, 1981).

49 Relatively few studies have measured performance at a large scale to distinguish  
50 between underlying shapes and phenomena (Dell et al., 2011) (Dowd, King, & Denny,  
51 2015). The purpose of this study was to conduct a broad-scale comparative analysis  
52 of the performance of phenomenological and mechanistic models on thermal response

53 data.

## 54 **3 Methods**

### 55 **3.1 Data**

56 Metabolic trait data was derived from the BioTraits dataset accumulated by Dell *et*  
57 *al.*, (2011) . This included approximately 2,445 intraspecific temperature responses for  
58 growth, respiration and photosynthesis rates in plants and bacteria from terrestrial and  
59 aquatic environments. TPCs with positive and non zero trait values were selected and  
60 those with 6 or more observations were included in the analysis. A minimum of 6 data  
61 points was chosen in order to successfully fit the full Schoolfield model which requires  
62 at least 6 observations. A total of 1,577 TPCs were fitted with both phenomenological  
63 and mechanistic models to assess the effect of temperature on biological trait values.  
64 The data for analysis were subsetting and exported using Python 3.6.7, the pandas and  
65 numpy libraries.

### 66 **3.2 Model fitting**

#### 67 **3.2.1 Phenomenological Models**

68 Two different phenomenological models were used in this study. A generic cubic poly-  
69 nomial model was fit to each TPC using Ordinary Least Squares as it is often used to  
70 describe unimodal data.

$$\beta = \beta_0 + \beta_1 T + \beta_2 T^2 + \beta_3 T^3 \quad (1)$$

71  $\beta$ , is the trait of interest (respiration, growth or photosynthesis),  $T$  is temperature  
72 ( $^{\circ}\text{C}$ ) and  $\beta_0$ ,  $\beta_1$ ,  $\beta_2$  and  $\beta_3$  are coefficients of the function lacking any mechanistic  
73 interpretation.

74 Briere's model is a 3 parameter model that describes the non-linear relationship  
75 of developmental rates for insect species (Briere *et al.*, 1999). This empirical func-  
76 tion was used as it accounts for upper and lower temperature thresholds, asymmetry  
77 about the optimum temperature, presence of an inflection point and a sharp decline in  
78 developmental rate above optimum temperature.

$$\beta = \beta_0 T(T - T_0) \sqrt{T_m - T} \quad (2)$$

79  $\beta$  represents the trait value where  $T_0$  is the minimum feasible temperature ( $^{\circ}\text{C}$ ) and  
80  $T_m$  is the maximum temperature ( $^{\circ}\text{C}$ ) that a trait can withstand before going to 0  
81  $^{\circ}\text{C}$ .  $\beta_0$  is the normalization constant and was initialized as 1 for TPC fitting.  $T_0$  was  
82 estimated as the minimum temperature and  $T_m$  as the maximum temperature recorded  
83 for each TPC.

### 84 3.2.2 Mechanistic Models

85 The mechanistic models fitted were variations of the Schoolfield model based on ther-  
86 modynamics and enzyme kinetics (?, ?). The full model contains 6 parameters including  
87 both high and low deactivation energy.

$$\beta = \frac{\beta_0 e^{-\frac{E}{k}(\frac{1}{T} - \frac{1}{283.15})}}{1 + e^{\frac{E_l}{k}(\frac{1}{T_l} - \frac{1}{T})} + e^{\frac{E_h}{k}(\frac{1}{T_h} - \frac{1}{T})}} \quad (3)$$

88  $k$  is the Boltzmann constant ( $8.617 \times 10^{-5}$  eV  $\text{K}^{-1}$ ).  $\beta$  represents the  
89 value of the trait at a given temperature ( $T$ ) in Kelvin ( $\text{K} = ^{\circ}\text{C} + 273.15$ ).  $\beta_0$  is the  
90 trait value that corresponded to the temperature closest to 278.15 K ( $5^{\circ}\text{C}$ ), controlling  
91 the vertical offset of the curve.  $E$  is the activation energy (eV) and controls the rise of  
92 the curve up to the peak in the normal operating range for the enzyme.  $E_l$  is  
93 the enzyme's low-temperature de-activation energy (eV) which controls the behavior of  
94 the enzyme (and the curve) at very low temperatures while  $E_h$  is the enzyme's high-

95 temperature de-activation energy (eV), controlling the behavior of the enzyme at very  
 96 high temperatures.  $T_l$  is the temperature at which the enzyme is 50% low-temperature  
 97 deactivated and  $T_h$  is the temperature at which the enzyme is 50% high-temperature  
 98 deactivated. The simplified models are similar to the full model disregarding either  
 99 high temperature (4) or low temperature deactivation (5):

$$\beta = \frac{\beta_0 e^{\frac{-E}{k}(\frac{1}{T} - \frac{1}{283.15})}}{1 + e^{\frac{E_l}{k}(\frac{1}{T_l} - \frac{1}{T})}} \quad (4)$$

$$\beta = \frac{\beta_0 e^{\frac{-E}{k}(\frac{1}{T} - \frac{1}{283.15})}}{1 + e^{\frac{E_h}{k}(\frac{1}{T_h} - \frac{1}{T})}} \quad (5)$$

100  $\beta_0$  was initialized as the untransformed trait value corresponding to the temperature  
 101 closest to 278.15 K (5°C). From here, each TPC was divided into two sections either side  
 102 of the peak. The peak was calculated as the highest trait value and it's corresponding  
 103 temperature. The first section, or left hand side of the curve, comprised of temperatures  
 104 and their corresponding trait values below the peak while the second section, or right  
 105 hand side of the curve, contained values above the peak. For each section, temperature  
 106 data were multiplied by 1/k and trait values logged. A linear regression was then fit  
 107 to the data and starting parameter estimates were calculated. For the left hand side of  
 108 the curve, below the peak,  $E$  was calculated as the absolute value of the slope of the  
 109 line.  $T_l$  was recorded as the temperature (transformed from 1/kt to K) from which the  
 110 mean logged trait value was taken and the 1/kt value calculated from the regression  
 111 line.  $E_l$  was assumed to be half the value of  $E$ . For the left hand side of the curve,  
 112 below the peak,  $E_h$  was recorded as the slope of the line and  $T_h$  was estimated similar  
 113 to  $T_l$ . For cases in which above or below peak data contained 1 point or were absent,  
 114  $E$  was initialized as 0.65 and  $E_h$  as 3 times  $E$  to reflect a sharper slope as trait values  
 115 decline with increasing temperature.  $T_l$  was estimated as the lowest tempertaure and  
 116  $T_h$  as the maximum temperture.

117 Apart from the cubic model, all models were fit in R Studio 3.2.3 using non-linear  
118 least squares methods. The nlsLM function was used to incorporate the Levenberg-  
119 Marquardt fitting algorithm, returning a vector of weighted residuals whose sum of  
120 square was minimized (R documentation). Parameters were bounded and optimized  
121 within the function. Estimated starting parameters for all 3 Schoolfield models were fit-  
122 ted and then randomized with a gaussian fluctuation before re-fitting. Each Schoolfield  
123 model was fitted to the TPC 20 times, once with the original estimated parameters  
124 and 19 times with starting values randomly sampled from a gaussian distribution with  
125 a mean of the calculated parameter and distribution of 0.05. The convergence rate was  
126 recorded as the number of successful fits achieved out of a total of 20 attempts.

### 127 **3.3 Model Selection**

128 Models with the best fit for each individual TPC were defined as those with the lowest  
129 Akaike Information Criterion  $\Delta AIC_c$  score.  $AIC_c$ , a second order derivative of the  
130 original  $AIC$ , contains a bias correction term for small sample size and is suggested as  
131 an appropriate selection tool when the number of parameters exceed  $n/40$ ,  $n$  referring  
132 to sample size (B Johnson & Omland, 2004).  $AIC$  or  $AIC_c$  is often used to find the  
133 best approximating model to the unknown data as it accounts for the sum of squares,  
134 goodness-of-fit measure, and varying numbers of parameters (Burnham & Anderson,  
135 2002). The original  $AIC$  equation, used in calculating  $AIC_c$  is as follows;

$$AIC = -2\log(\mathcal{L}(\hat{\theta} | y)) + 2k \quad (6)$$

136 where  $\mathcal{L}(\hat{\theta} | y)$  is the log-likelihood at it's maximum point, corresponding to the  
137 probability of the data given a model.  $k$  is defined as the number of free parameters  
138 in the model. An alternative formula to calculate  $AIC_c$ , proposed by Hurvich & Tsai  
139 (1989), was used to prevent values tending to infinity;



$$AIC_c = AIC + \frac{2k(k+1)(k+2)}{\max(n, k+3) - k - 2} \quad (7)$$

140  $k$  is the number of parameters in the fitted model and  $n$  the number of observations.  
 141 For phenomenological models which were not fit with varying starting parameters, the  
 142 best model was taken as that with the lowest  $AIC_c$ . When fitting the mechanistic  
 143 models  $AIC_c$ , was rescaled to  $\Delta AIC_c$  using the following equation;

$$\Delta_i = AIC_{ci} - AIC_{cmin} \quad (8)$$

144  $AIC_{ci}$  is the  $AIC_c$  for the  $i$ th model and  $AIC_{cmin}$  is the minimum  $AIC_c$  among  
 145 all models. The larger  $\Delta_i$ , the weaker the model. The best model was considered to  
 146 be the model in which  $\Delta AIC$  was equal to 0 (minimum  $\Delta AIC$  score in the TPC)  
 147 (P Burnham & R Anderson, 2004). Each TPC was then plotted with the best selected  
 148 fit per model and analyzed visually. An Akaike weight,  $W_i (AIC_c)$ , was used for  
 149 model averaging, representing the probability that the model chosen is the best model  
 150 for the observed data.

$$W_i = \frac{\exp(-\Delta_i/2)}{\sum_{r=1}^R \exp(-\Delta_r/2)} \quad (9)$$

151  $W_i$  is the weight of evidence in favour of the model. These depend on the full set  
 152 of models and must sum to 1.  $R$  in the denominator incorporates the summation of all  
 153  $AIC_c$  weights to generate this ratio.

## 154 4 Results

155 A total of 1,577 TPCs were analyzed following data manipulation. The sample size  
 156 per TPC did not follow a normal distribution, ranging from 6 to 637 samples with a  
 157 median value of 8. 75% of curves contained 13 values or less (see Appendix 1.1). Both

phenomenological and mechanistic models fit the majority of the data, as seen in table 1, with Cubic and Briere fitting all curves compared to the Schoolfield models. Among the mechanistic models, those simplified with fewer parameters (S1 and S2) achieved a greater number of fits. Convergence was defined as the proportion of fits out of 20 attempts for each Schoolfield model. The high energy deactivation Schoolfield model (S1) converged more on average compared to the full Schoolfield model which had the lowest convergence rate.

165

Table 1: Number of successful model fits and proportion per model type for each Temperature Performance Curve across the entire dataset. Convergence rate, average number of successful fits out of 20 attempts, also included for all Schoolfield models.

	Cubic	Briere	S1	S2	S3
Number	1577	1368	1426	1432	1270
Proportion	100%	87%	90%	91%	81%
Convergence	-	-	77%	75%	68%

Upon visual inspection of TPCs, mechanistic models S1 and S3, often demonstrated a good fit and successfully captured the gradual rise and sharp fall of full TPC curves. The low temperature deactivation Schoolfield model (S2) was in general insufficient at fitting to the observed data. Briere was suitable for full TPCs but did not always fit curves outside of this trend. Both Briere and the Schoolfield models however were not as flexible as the Cubic model which fit to more TPCs, often demonstrating a roughly good fit. Figure 1, illustrates the range of fits achieved for a full TPC. Table 2 confirms that Briere provided the best fit for subfigure (a) followed by the Cubic model and S1 which had the lowest  $\Delta AIC_c$  out of the mechanistic models. S1 was the best fitting model for subfigure (b) also reflected in the accompanying  $\Delta AIC_c$ . According the table 2, Cubic would be the next best model which visually, is inaccurate.

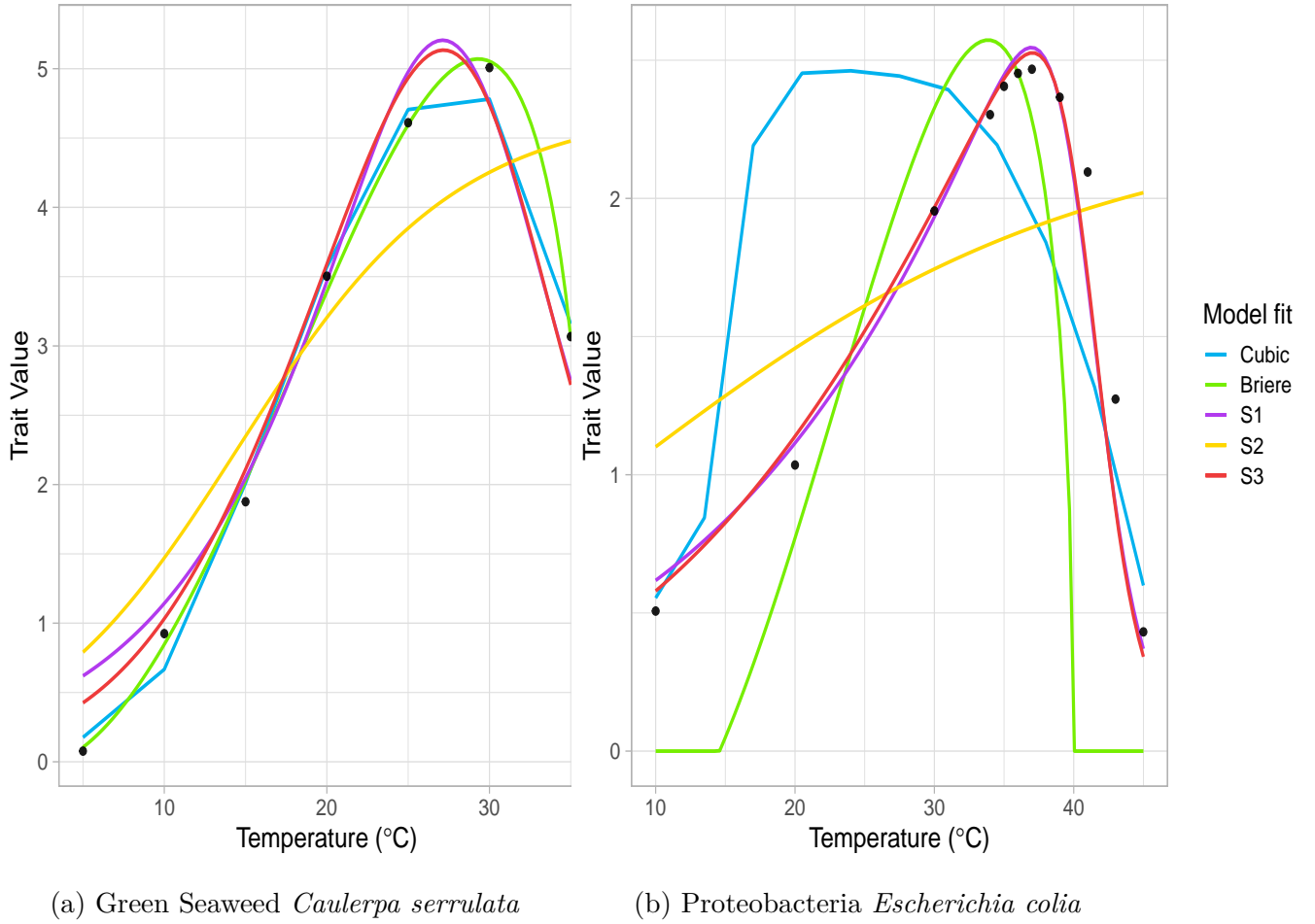


Figure 1: Two typical TPCs demonstrating all 5 models fit to observed data. a) All models captured data well, particularly Briere. b) Only the mechanistic models, particularly S1 and S3, come close to an optimal fit.

Table 2:  $\Delta AIC_c$  results for all models fitted to the TPCs in Figure 1.

TPC	Cubic	Briere	S1	S2	S3
a) Green Seaweed	21.73	-0.59	27.28	44.19	65.78
b) Proteobacteria	10.75	38.59	-4.62	43.68	23.11

Model performance was assessed by evaluating the proportion of best fitting models, according to their  $\Delta AIC_c$  value, across the entire dataset and between groups. In figure 2, it is evident that the Cubic model was selected most frequently as the best fitting

180 model, followed by the high temperature deactivation Schoolfield model (S1), Briere and  
 181 the remainder of the Schoolfield models. The low temperature deactivation Schoolfield  
 182 model had the lowest number of best fits within the overall dataset.

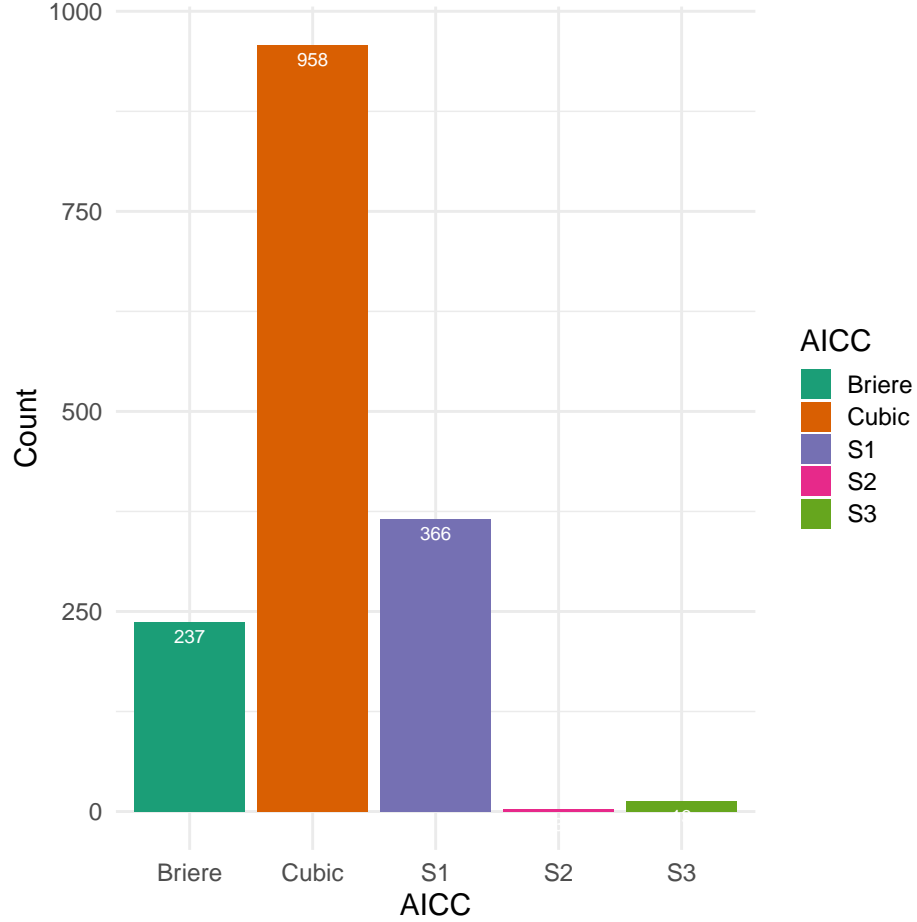


Figure 2: Number of times each model was selected as the best model per TPC, according to  $\Delta AIC_c$  score, within the entire dataset ( $n = 1577$ ).

183 Model performance was also assessed between different trait values which were  
 184 grouped under the following categories; Photosynthesis, Respiration and Growth. From  
 185 figure 3, it is evident that the cubic model comprised of the largest proportion of best  
 186 fits. The poorest performing models, S2 and S3, were only fit to growth and respiration  
 187 data.

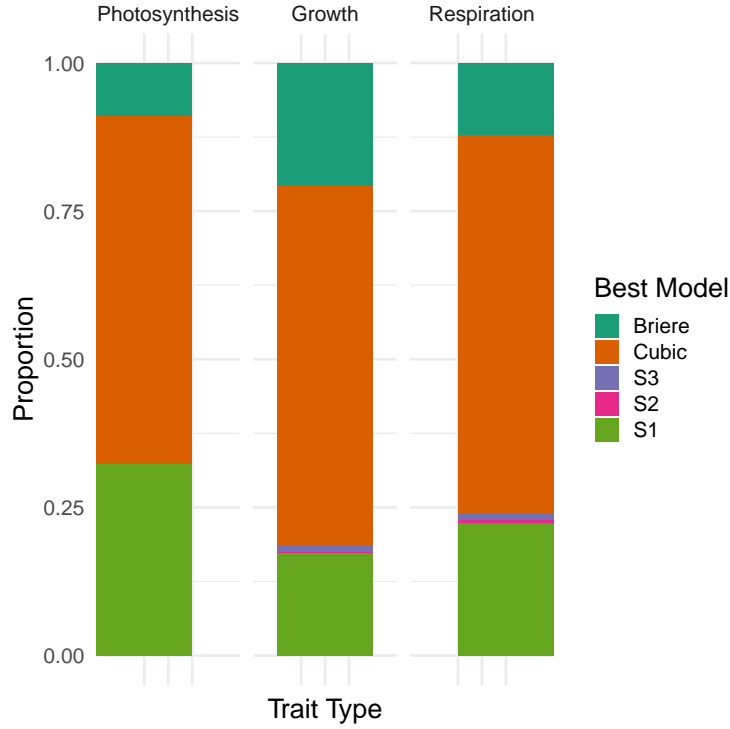


Figure 3: Proportion of best models selected for each trait type summarized into relative categories; Photosynthesis, Growth and Respiration. Best model was selected according to  $\Delta AIC_c$  score, within the entire dataset ( $n = 1577$ ).

188 In figure 4, the general pattern of model performance between kingdoms of con-  
 189 sumers was observed. The kingdoms Archae and Protozoa strongly favoured phe-  
 190 nomenological models; Cubic and Briere selected as the best models respectively. Pro-  
 191 tozoa was the only kingdom in which no mechanistic models provided the best fit. Apart  
 192 from the high temperature deactivation Schoolfield model across all other kingdoms, the  
 193 best fits for the low temperature deactivation and full Schoolfield model were present  
 194 only in Bacteria and Plantae.

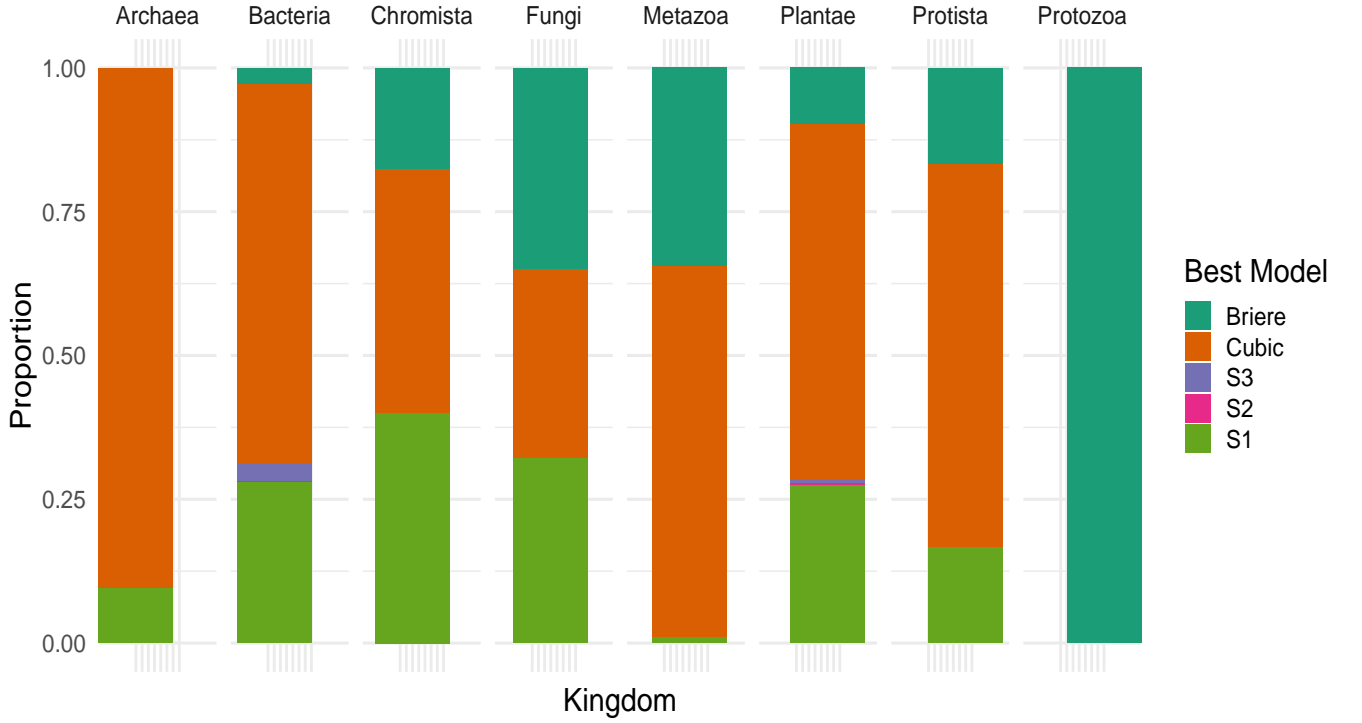


Figure 4: Proportion of best models selected for each Kingdom of consumers. Best model was selected according to  $\Delta AIC_c$  score, within the entire dataset ( $n = 1577$ ).

195 The evidence for the strength of fit for each model was calculated by categorizing  
 196  $\Delta AIC_c$  scores according to guidelines adapted by Burnham & Anderson (2004); models  
 197 with  $\Delta AIC_c \leq 2$  show substantial support; those in which  $4 \leq \Delta AIC_c \leq 7$  have consid-  
 198 erably less support; and those with  $\Delta AIC_c > 10$  have no support. In table 3, strength of  
 199 fit was investigated for TPCs in which all models fit the observed data. It is clear that  
 200 the Cubic model out-performed other models two to three times over in which it had the  
 201 strongest supporting evidence. The high temperature deactivation Schoolfield model  
 202 comprised of a relatively large proportion of strongly supported models in comparison  
 203 to the remaining models. The low temperature deactivation energy and full Schoolfield  
 204 models (S2 and S3) had little to no support. This is reflected in  $AIC_c$  weights (figure 5)  
 205 with the cubic model possessing a greater proportion of higher weights, followed by the  
 206 simplified Schoolfield high energy deactivation model (S1). Both models demonstrate

207 a higher probability of being the model that best describes the data.

Table 3:  $\Delta AIC_c$  scores TPCs in which all models converged. Scores fall into respective categories as per the recommended guidelines. Categories represent strength of fit, with lower  $\Delta AIC_c$  indicative of supportive evidence in favour of the model ( $n = 1156$ ).

Model	$\Delta < 2$	$2 < \Delta \leq 4$	$4 < \Delta \leq 7$	$7 < \Delta \leq 10$	$\Delta > 10$
Cubic	1100	88	117	84	188
Briere	275	47	79	62	905
S1	520	125	198	169	414
S2	51	49	89	111	1132
S3	13	4	6	8	1239

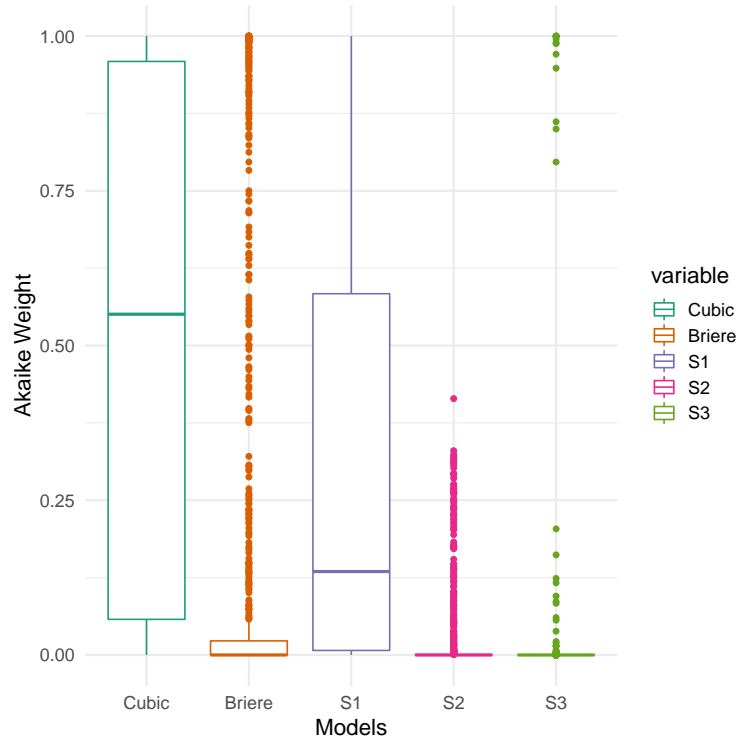


Figure 5: Distribution of Akaike weights for each model. Weightages were calculated for TPCs in which all models converged ( $n = 1156$ ).

## 5 Discussion

Which model is 'best'? At first, the answer may seem straightforward but on further inspection this is not the case, comparing alternative models that make different simplifications with a common biological assumption (Levins, 1966). The goal of non-linear regression is to minimize the sum-of-squares and so it appears that the model with the smallest value is best. However, this is often not applicable when models have varying numbers of parameters, and therefore different inflection points. Any method to compare a simple model with a more complicated one must balance the decrease in sum-of-squares with the increase in the number of parameters. From analyzing the data, it is clear that the Cubic model was generally the better fitting model within the dataset and between traits and Kingdoms. This is possibly due to model flexibility as phenomenological models are not constrained by parameter assumptions. However, this provides little information about the variation in thermal physiology among organisms and so prevents any biological interpretation.

Mechanistic models are preferable in order to understand the thermal ecology and metabolic adaptations of organisms as well as generate testable predictions for future studies (Peek, Russek-Cohen, D Wait, & N Forseth, 2002)(Schulte, 2015) (Martin et al., 2017) (DeLong et al., 2017). The best fitting mechanistic model was the Schoolfield high temperature deactivation model (S1) which may be a consequence of experimental limitations (?, ?), for example if organisms have only been studied over part of the temperature spectrum. Compared to S2 and S3, which both contain low temperature deactivation parameters, S1 performed significantly better. This may be due TPCs containing higher temperature values and/or to the fact that low temperature deactivation is difficult to detect (Pawar, Dell, Savage, & Knies, 2016).

Another plausible explanation for observed model performance lies in the calculated parameter estimates. General assumptions applied to the entire dataset can lead to over



or underestimated values for individual TPCs. For example, the normalization constant  $\beta_0$ , which standardizes rate performance across groups, is particularly susceptible to overestimating trait values at the selected reference temperature (Kontopoulos, García-Carreras, Sal, Smith, & Pawar, 2018). Parameters such as  $T_h$  and  $T_l$  were also observed to be unrealistic in certain datasets. The mean activation energy for each model was close to the reported activation energy of 0.65 eV with S1 having the closest mean value. Parameters were bound and optimized using the Levenberg-Marquardt algorithm as part of nlsLM function which is the virtual standard in optimization. However this approach is not immune to faults with a generally slow convergence rate and probability of getting lost in parameter space (K. Transtrum & Sethna, 2012).

Model selection was chosen on the basis of fit and complexity to compare all models simultaneously using *AIC*. Instead of the hypothesis testing approach, associated with the likelihood ratio test, or  $R^2$  measure of fit which is inappropriate for non-linear regression (?, ?), *AIC* combines the Kullback-Leiber distance, measure of discrepancy, and Fisher’s maximized log-likelihood to select a parsimonious model to analyze empirical data (Akaike, 1998). Even in moderate sample sizes, the second order derivative  $AIC_c$  provides substantially better model selections than *AIC* (Hurvich & Tsai, 1991). One major disadvantage to this approach was that values tended to infinity when the sample size,  $n$ , was equal to the number of parameters,  $k + 1$ , which occurred for the full Schoolfield model ( $k = 6$ ). An alternative formula was used to avoid omitting data but is not well explored in the literature.

## References

- Akaike, H. (1998). Information theory and an extension of the maximum likelihood principle. In *Selected papers of hirotugu akaike* (pp. 199–213). Springer.
- Bernardo, J., & Spotila, J. R. (2006). Physiological constraints on organismal response

259 to global warming: mechanistic insights from clinally varying populations and  
 260 implications for assessing endangerment. *Biology Letters*, 2(1), 135-139. doi:  
 261 10.1098/rsbl.2005.0417

262 B Johnson, J., & Omland, K. (2004, 03). Johnson jb, omland ks.. model selection in  
 263 ecology and evolution. trends ecol evol 19: 101-108. *Trends in ecology evolution*,  
 264 19, 101-8. doi: 10.1016/j.tree.2003.10.013

265 Burnham, K. P., & Anderson, D. R. (2002). *Model selection and multimodel inference:*  
 266 *a practical information-theoretic approach* (2nd ed.). Springer.

267 Dell, A. I., Pawar, S., & Savage, V. M. (n.d.). The thermal depen-  
 268 dence of biological traits. *Ecology*, 94(5), 1205-1206. Retrieved from  
 269 <https://esajournals.onlinelibrary.wiley.com/doi/abs/10.1890/12-2060.1>  
 270 doi: 10.1890/12-2060.1

271 Dell, A. I., Pawar, S., & Savage, V. M. (2011). Systematic variation in the  
 272 temperature dependence of physiological and ecological traits. *Proceedings*  
 273 *of the National Academy of Sciences*, 108(26), 10591-10596. Retrieved from  
 274 <https://app.dimensions.ai/details/publication/pub.1026914980> and  
 275 <http://www.pnas.org/content/108/26/10591.full.pdf> (Exported from  
 276 <https://app.dimensions.ai> on 2019/03/04) doi: 10.1073/pnas.1015178108

277 DeLong, J. P., Gibert, J. P., Luhring, T. M., Bachman, G., Reed, B., Neyer, A., &  
 278 Montooth, K. (2017). The combined effects of reactant kinetics and enzyme  
 279 stability explain the temperature dependence of metabolic rates. *Ecology and*  
 280 *evolution*, 7(11), 3940-3950.

281 Dowd, W. W., King, F. A., & Denny, M. W. (2015). Thermal vari-  
 282 ation, thermal extremes and the physiological performance of individu-  
 283 als. *Journal of Experimental Biology*, 218(12), 1956-1967. Retrieved from  
 284 <http://jeb.biologists.org/content/218/12/1956> doi: 10.1242/jeb.114926

285 Fangue, N. A., Healy, T. M., & Schulte, P. M. (2011, 08). Thermal Perfor-

286 mance Curves, Phenotypic Plasticity, and the Time Scales of Temperature Ex-  
 287 posure. *Integrative and Comparative Biology*, 51(5), 691-702. Retrieved from  
 288 <https://dx.doi.org/10.1093/icb/icr097> doi: 10.1093/icb/icr097  
 289 Hurvich, C. M., & Tsai, C.-L. (1991, 09). Bias of the corrected AIC criterion  
 290 for underfitted regression and time series models. *Biometrika*, 78(3), 499-  
 291 509. Retrieved from <https://dx.doi.org/10.1093/biomet/78.3.499> doi:  
 292 10.1093/biomet/78.3.499  
 293 Kontopoulou, D.-G., García-Carreras, B., Sal, S., Smith, T. P., & Pawar, S. (2018). Use  
 294 and misuse of temperature normalisation in meta-analyses of thermal responses  
 295 of biological traits. *PeerJ*, 6, e4363.  
 296 K. Transtrum, M., & Sethna, J. (2012, 01). Improvements to the levenberg-marquardt  
 297 algorithm for nonlinear least-squares minimization.  
 298 Levins, R. (1966, 01). The strategy of model building in population biology. *Am. Sci.*,  
 299 54, 421-431.  
 300 Low-Dălcăre, E., Boatman, T. G., Bennett, N., Passfield, W., Gavalăş-  
 301 Olea, A., Siegel, P., & Geider, R. J. (n.d.). Predictions of re-  
 302 sponse to temperature are contingent on model choice and data qual-  
 303 ity. *Ecology and Evolution*, 7(23), 10467-10481. Retrieved from  
 304 <https://onlinelibrary.wiley.com/doi/abs/10.1002/ece3.3576> doi:  
 305 10.1002/ece3.3576  
 306 Martin, B. T., Pike, A., John, S. N., Hamda, N., Roberts, J., Lindley, S. T., & Danner,  
 307 E. M. (2017). Phenomenological vs. biophysical models of thermal stress in  
 308 aquatic eggs. *Ecology letters*, 20 1, 50-59.  
 309 Non-linear regression of biological temperature-dependent rate mod-  
 310 els based on absolute reaction-rate theory. (1981). *Jour-*  
 311 *nal of Theoretical Biology*, 88(4), 719 - 731. Retrieved from  
 312 <http://www.sciencedirect.com/science/article/pii/0022519381902460>",

313 author = "R.M. Schoolfield and P.J.H. Sharpe and C.E. Magnuson",  
 314 abstract = "Biological temperature-dependent rate models based on  
 315 Arrhenius' and Eyring's equations have been formulated by Johnson  
 316 Lewin (1946), Hultin (1955), and Sharpe DeMichele (1977). The  
 317 original formulation of Sharpe and DeMichele is poorly suited  
 318 for non-linear regression. Very high correlations of parameter  
 319 estimators occassionally make regression with their equation  
 320 impossible using Marquardt's algorithm (1963). This analysis  
 321 describes a new formulation of Sharpe and DeMichele's model that  
 322 greatly alleviates the non-linear regression problem. It is partly  
 323 based on Hultin's formulation (1955). Biological and graphical  
 324 interpretation of the model parameters is discussed. Regression  
 325 suitability is illustrated with a typical data set. Similar  
 326 modifications to the equations of Hultin (1955) and Johnson Lewin  
 327 (1946) are described doi: [https://doi.org/10.1016/0022-5193\(81\)90246-0](https://doi.org/10.1016/0022-5193(81)90246-0)  
 328 O.Hoegh-Guldberg, Jacob, Taylor, Bindi, Brown, Camilloni, ... Zhou (2018). Impacts  
 329 of 1.5°C global warming on natural and human systems. an ipcc special report on  
 330 the impacts of global warming of 1.5°C above pre-industrial levels and related  
 331 global greenhouse gas emission pathways, in the context of strengthening the  
 332 global response to the threat of climate change, sustainable development, and  
 333 efforts to eradicate poverty..  
 334 Pawar, S., Dell, A. I., Savage, V. M., & Knies, J. L. (2016). Real versus artificial  
 335 variation in the thermal sensitivity of biological traits. *The American Naturalist*,  
 336 187(2), E41–E52.  
 337 P Burnham, K., & R Anderson, D. (2004, 01). Multimodel inference: understanding  
 338 aic and bic in model selection. *Sociological Methods Research*, 33, 261-304.  
 339 Peek, M., Russek-Cohen, E., D Wait, A., & N Forseth, I. (2002, 07). Physiological

340 response curve analysis using nonlinear mixed models. *Oecologia*, 132, 175-180.  
 341 doi: 10.1007/s00442-002-0954-0  
 342 Pracros, P., Briere, J.-F., Le Roux, A.-Y., & Pierre, J.-S. (1999, 02).  
 343 A Novel Rate Model of Temperature-Dependent Development for Arthro-  
 344 pods. *Environmental Entomology*, 28(1), 22-29. Retrieved from  
 345 <https://dx.doi.org/10.1093/ee/28.1.22> doi: 10.1093/ee/28.1.22  
 346 Quinn, B. K. (2017). A critical review of the use and performance of different func-  
 347 tion types for modeling temperature-dependent development of arthropod larvae.  
 348 *Journal of thermal biology*, 63, 65-77.  
 349 Schneider, E. D., & Kay, J. J. (2007). Order from disorder : The thermodynamics of  
 350 complexity in biology..  
 351 Schulte, P. M. (2015). The effects of temperature on aerobic metabolism: towards a  
 352 mechanistic understanding of the responses of ectotherms to a changing environ-  
 353 ment. *The Journal of experimental biology*, 218 Pt 12, 1856-66.

## 6 Appendices

### 6.0.1 Appendix 1

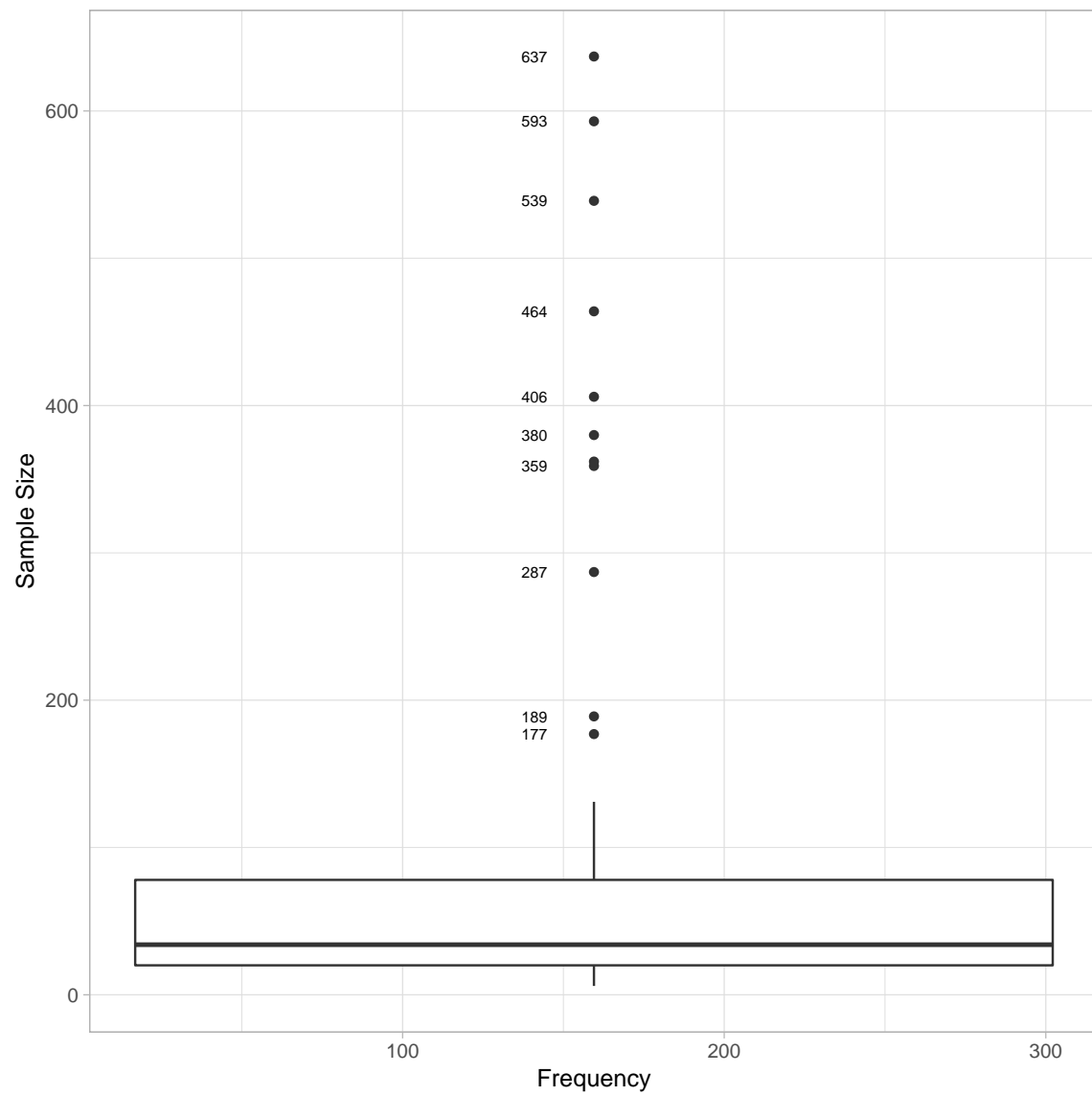


Figure 6: Boxplot illustrating the range of observations per Thermal Performance Curve. Outliers are labelled